Konya Mühendislik Bilimleri Dergisi, c. 10, s. 3, 774-792, 2022
Konya Journal of Engineering Sciences, v. 10, n. 3, 774-792, 2022
ISSN: 2667-8055 (Electronic)
DOI: 10.36306/konjes.1104000

THE POSSIBLE THERAPEUTIC IMPACTS OF PHOTOBIOMODULATION AND LOW-DOSE PHOTODYNAMIC THERAPY ON HUVECS TOWARDS ANGIOGENESIS: *A COMPARATIVE IN VITRO ANALYSIS*

[1]Dilara PORTAKAL KOÇ, [2]Günnur PULAT, [3]Nermin TOPALOĞLU

[1,2]Izmir Katip Celebi University, Department of Biomedical Technologies, Graduate School of Natural and Applied Sciences, Izmir, TURKIYE
[3]Izmir Katip Celebi University, Faculty of Engineering and Architecture, Department of Biomedical Engineering, İzmir, TURKIYE
[1]dilara@live.de, [2]gunnur.onak@ikcu.edu.tr, [3]nermin.topaloglu@ikcu.edu.tr

Geliş/Received: 15.04.2022; Kabul/Accepted in Revised Form: 09.08.2022

ABSTRACT: Photobiomodulation (PBM) is a non-ionizing therapy that promotes faster wound healing and cell proliferation/differentiation. It is recently understood that photodynamic therapy (PDT) may act as PBM when applied at low-level. In this study, a comparative analysis between PBM and low-dose PDT was performed on HUVECs to increase angiogenesis. HUVECs were irradiated at 808-nm of wavelength. Indocyanine green was used as a photosensitizer in PDT applications. Single and triple treatments were employed for both modalities. Their effects were analyzed with cell viability, intracellular ROS, MMP change, NO release, and morphological analysis. The expressions of vascularization-related proteins (VEGF, PECAM-1, and vWf) were determined through immunofluorescence staining and qRT-PCR. Temperature changes during applications were monitored to determine any thermal damages. It was observed that triple PDT application was more successful at increasing cell proliferation and tube-like structure formation with a 20% rate. The level of ROS did not significantly change in all applications. However, the amount of NO release in triple PDT application was nearly 5 times that of the control group, which showed it acted as a key molecule. The vascularization-related proteins were more strongly expressed in PDT applications. It was understood that low-dose PDT can exert a photobiomodulation effect to accelerate vascularization through NO release.

Keywords: *Photobiomodulation, Photodynamic therapy, 808-nm, Indocyanine green, HUVECs*

Fotobiyomodülasyon ve Düşük Doz Fotodinamik Terapinin HUVEC Hücrelerindeki Anjiyogenez'e Yönelik Olası Terapötik Etkileri: *Karşılaştırmalı İn Vitro Analiz*

ÖZ: Fotobiyomodülasyon (FBM), yara iyileşmesi, hücre proliferasyonu/farklılaşması mekanizmalarını hızlandıran iyonlaştırıcı olmayan bir ışık terapisidir. Son zamanlarda, fotodinamik terapinin (FDT) düşük dozlarda uygulandığında FBM gibi davranabileceği anlaşılmıştır. Bu çalışmada karşılaştırmalı bir analizle anjiyogenezi artırmak için HUVEC'ler üzerinde FBM ve düşük doz FDT'nin etkisi araştırılmıştır. HUVEC'ler 808 nm dalgaboyu ile uyarılmıştır. FDT uygulamalarında fotosensitizan olarak indosiyanin yeşil kullanılmıştır. Her iki yöntem tekli ve üçlü olarak uygulanmıştır. Uygulamaların etkileri hücre canlılığı, hücre içi ROS, MMP değişikliği, NO salınımı ve morfolojik analizler ile incelenmiştir. Vaskülarizasyonla ilgili proteinlerin (VEGF, PECAM-1 ve vWf) ifadeleri, immünofloresan boyama ve qRT-PCR yöntemleri ile belirlenmiştir. Olası termal hasarları belirlemek için ışık uygulamaları sırasındaki sıcaklık değişimleri izlenmiştir. Sonucunda, üçlü düşük doz FDT uygulamasının hücre proliferasyonu ve damar benzeri yapı oluşumunda %20 oranında daha başarılı olduğu gözlenmiştir. Bütün uygulamalarda ROS seviyesi önemli ölçüde değişmezken, üçlü FDT uygulamalarında NO salınımının miktarı kontrol grubunun yaklaşık 5 katı olmuş, bu da NO salınımının bu mekanizmada anahtar bir molekül olarak

hareket ettiğini göstermiştir. Vaskülarizasyonla ilgili proteinler de FDT uygulamalarında daha güçlü bir şekilde ifade edilmiştir. Sonuç olarak, düşük doz FDT'nin NO salınımı yoluyla vaskülarizasyonu hızlandırmak için fotobiyomodülatif etki gösterdiği anlaşılmıştır.

Anahtar Kelimeler: *Fotobiyomodulasyon, Fotodinamik terapi, 808-nm, İndosiyanin yeşil, HUVEC hücreleri*

1. INTRODUCTION

Light therapies are important strategies to combat cancerous and non-cancerous diseases and also to accelerate healing processes recently. Specifically, photodynamic therapy (PDT) is used to destroy cancer or bacterial cells and photobiomodulation (PBM) is used to enhance cell proliferation/differentiation, wound healing, and pain relief [Topaloglu and Bakay, 2022; Topaloglu *et al*., 2021a; Topaloglu *et al*., 2021b]. PBM is a non-ionizing and non-thermal light application that triggers some biochemical reactions inside the cells via mitochondria at visible and near-infrared wavelengths [Amaroli *et al*., 2019; de Freitas and Hamblin, 2016; Huang, 2009]. After the absorption of the low-level visible or near-infrared light by the target tissue, numerous biological functions are enhanced without causing any harm to the target [Hamblin, 2018]. The biological functions are associated with intracellular reactive oxygen species (ROS) production, adenosine triphosphate (ATP) generation, nitric oxide (NO) release, DNA synthesis, etc. [Hawkins *et al*., 2005]. Cytochrome c oxidase (COX) is an important part of the electron transport chain in mitochondria [Hough *et al*., 2014] and acts as a chromophore for visible and near-infrared light during PBM applications which results in a protein gradient across the cell and mitochondrial membrane [Zorov *et al*., 2014]. This process causes an increase in mitochondrial membrane potential (MMP) change followed by ATP synthesis, intracellular ROS generation, and nitric oxide (NO) release [Hamblin, 2018]. Released NO molecules and produced intracellular ROS are key molecules that mediate the mechanism of PBM and serve as signaling molecules to influence many physiological pathways that will end up with the therapeutic outcome of PBM [Zhang *et al*., 2016; Mittal *et al*., 2014]. COX is inhibited by NO molecules. When it is released from COX after light absorption, it will influence the respiration rate in the cells. This is the reason why ATP synthesis increases and other therapeutic outcomes such as cell proliferation/differentiation can be obtained in the cells treated with PBM [Beltrán *et al*., 2000; Karu *et al*., 2005; Borutaite *et al*., 2000].

PDT is also a therapeutic light application that is generally used to destroy pathogens or cancer cells in the presence of a photosensitizer. Visible or near-infrared light is applied to excite the photosensitizer and a chain of transfer reactions occurs to produce a high concentration of ROS that will exhibit photo-cytotoxicity on unwanted cells [Castano *et al*., 2004]. The quantum oxygen yield of a photosensitizer upon irradiation will determine the efficacy of PDT. Higher ROS yield will determine the degree of the killing effect of PDT. Lower ROS yield may not exhibit cytotoxicity and may even induce cell survival mechanisms in the cells [Topaloglu *et al*., 2016]. PDT which was used at low doses induced cell proliferation and VEGF expression in nude mice brains in a previous study [Zhang *et al*., 2005]. Thus, it was understood that the optimization of the light parameters in these light applications is very important to obtain the desired outcome of the applications and PDT at a low level may be used to enhance cell proliferation/differentiation and wound healing [Topaloglu *et al*., 2016; Topaloglu *et al*., 2015]. This information has opened new perspectives to the use of PDT for different strategies, instead of antibacterial or anticancer purposes. The biphasic dose-response of the cells towards PDT can be utilized and the potential of PDT to produce ROS in a controllable way can be an advantageous tool to induce cell proliferation/differentiation, wound healing, etc [Topaloglu and Bakay, 2022]. In PBM, the chromophore is the COX in mitochondria and its prevalence may determine its effectiveness [Topaloglu *et al*., 2021a]. In PDT, photosensitizers act as a chromophore which is administered exogenously. Thus, its concentration can be easily adjusted depending on the application type and desired outcome [Topaloglu and Bakay, 2022].

Recently, there have been several studies that used PDT as a stimulative tool. Bolukbasi Ates and their colleagues used 809-nm of wavelength in the presence of indocyanine green (ICG) to enhance the

osteogenic differentiation at low energy densities and ICG concentrations [Ateş *et al*., 2018]. Topaloglu and Bakay used chlorin e6 (Ce6) and red light to enhance neural cell differentiation, again at low-level light parameters and photosensitizer concentration [Topaloglu and Bakay, 2022]. Another study that was performed on scratched wounds of fibroblasts showed that 660-nm of wavelength in the presence of 5-ALA induces faster wound healing [Sibata *et al*., 2000]. In light of these studies, it was understood that low-dose PDT may serve a stimulative effect and may become more successful than PBM by choosing the appropriate parameters more properly.

Endothelial cells have diverse functions and perform many important duties in the body. Mainly, they are responsible for the repair of the biological tissue and new blood vessel formation depending on their large capacity to divide, migrate, and differentiate for building vessels through angiogenesis. Human umbilical vein endothelial cells (HUVEC) are obtained from the vessel of the umbilical cord and are good sources to study the behavior of the endothelial cells [Terena *et al*., 2021]. It is also very valuable to analyze the photobiomodulation effect of light on these cells to reveal their potential for angiogenesis upon irradiation. Thus, the comparative analysis of PBM and low-dose PDT was performed on HUVECs in this study. Besides, the potential of 808-nm of wavelength was analyzed in PBM and low-dose PDT because of the deep penetration capacity of NIR light into the biological tissue. The most appropriate photosensitizer that strongly absorbs the wavelengths around 800-nm is ICG [Topaloglu *et al*., 2015]. That's why ICG was used in low-dose PDT applications to compare its stimulative potential with PBM. To determine the effect of the PBM and low-dose PDT on HUVECs, cell viability, intracellular ROS, MMP change, NO release, and morphological analysis of HUVECs were performed. Besides, the expressions of important vascularization-related proteins were determined through immunofluorescence staining and qRT-PCR. Finally, the temperature change was monitored with a thermal camera to understand whether there was a thermal effect of NIR light irradiation on the cells.

2. MATERIALS AND METHODS

2.1 Light Source

In this study, an 808-nm diode laser (Teknofil, Istanbul, Turkey) was used as a light source with a maximum output power of 2 Watts. The optical fiber of the laser device was positioned vertically and the fiber tip was 10 cm distant from the cell culture plates on an optical table. The illumination area was adjusted to irradiate a definite area homogeneously on the cell culture plates. The output power was set to 600 mW and 1 J/cm^2 energy density was applied whether the application was PBM or low-dose PDT with an exposure duration of 5 seconds.

2.2 Cell Culture

Human umbilical vein endothelial cells (HUVECs) were kindly provided from the Animal Cell Culture and Tissue Engineering Laboratory, Ege University and cultured in a humidified atmosphere with 5% CO_2 at 37°C in Dulbecco's Modified Eagle's Medium (DMEM, Sigma-Aldrich, St. Louis, MO, USA) containing 5% fetal bovine serum (FBS, Gibco, Dublin, Ireland), 1% L-glutamine (Sigma-Aldrich, St. Louis, MO, USA) and 1% penicillin. After they reached 90% confluency, they were trypsinized to dissociate them from the flask, and then transferred to the wells of a 96-well plate where the cells received light irradiation. For PDT applications, 1x10^5 cells were seeded in a single well of the 96-well plate to prevent a significant amount of cell loss during the multiple washing steps after ICG incubation. For PBM applications, 1x10^4 cells were seeded in a single well of the 96-well plate. They were cultured for 24 hours at 37 °C before light applications.

2.3 Photosensitizer

For low-dose PDT applications, ICG was used as a photosensitizer because of its strong absorption band at around 800 nm of wavelength. 1.93 mg of ICG (Santa Cruz, Dallas, Texas, USA) was dissolved in 500 μL DMEM to prepare a stock solution with a concentration of 5 mM. Then it was diluted with DMEM to the concentrations of 0.05, 0.1, 0.25, 0.5, 1, 2.5, and 5 μM to be used in the analyses.

2.4 Cytotoxicity of the Photosensitizer on HUVECs

Seven different concentrations of ICG (0.05, 0.1, 0.25, 0.5, 1, 2.5, and 5 μM) were prepared in serum-free medium (DMEM) in the dark, incubated with HUVECs for 1 hour to observe the possible toxic effect of the photosensitizer on the cells, and finally to determine the ideal concentration for the low-dose PDT applications. After the incubation, the cells were washed once with phosphate-buffered saline (PBS, Sigma-Aldrich, St. Louis, MO, USA) and endothelial cell growth medium (EGM, Lonza, Basel, Switzerland) was added. After 24h, cell viability analysis was performed by 2, 5-diphenyl tetrazolium bromide (MTT, Sigma-Aldrich, St. Louis, MO, USA) measuring the absorbance with a microplate reader at 570 nm (Multimode Microplate Reader Biotek Synergy HTX, Biotek, Winooski, VT, USA).

2.5 Experimental Procedures of PBM and Low-Dose PDT

The effect of light applications in PBM and low-dose PDT therapies was investigated with two different modalities: single and triple light treatments. In the single light treatment modality, the cells were irradiated only once throughout the experiments. In the triple light treatment modality, the cells received daily irradiation with a time interval of 24 hours three times. Before the light irradiations, the cells were incubated with 0.1 μM ICG for 1 hour in low-dose PDT groups. When the incubation with ICG was completed, the cells were washed with PBS twice and then EGM was added to them. In the meantime, the cells in PBM groups were not incubated with ICG, only their medium was refreshed and EGM was added. Before laser applications, the optical table and the laser device were sterilized for 30 min under UV light. Then, the cells were irradiated by an 808-nm diode laser at 1 J/cm^2 energy density. To perform a triple light treatment, this application was repeated three times at 24-hour intervals. Besides the control group which did not receive any application, the ICG group was formed to investigate the effect of only ICG application on HUVECs and angiogenesis. The cells in this group were incubated with 0.1 μM ICG and were not irradiated with light. Similar to the light applications, ICG applications were performed as single and triple treatments. A set of cells in this group was incubated with ICG once and they were followed up for 7 days. The other set of cells in this group was incubated with ICG three times with a time interval of 24 hours and they were followed up for 7 days, too. The medium of HUVEC cells was refreshed with EGM every day.

2.6 Morphological Analysis of HUVECs

The morphology of HUVECs was evaluated microscopically throughout the experimental procedure on days 1, 2, 3, 4, and 7. An inverted microscope (Olympus CKX41, Olympus Co. Ltd., Tokyo, Japan) was used to capture microscopic images of the cells. For each sample at least 10 images were obtained with 20X magnification. When the tubular structures were formed during the follow-up period until day 7, the total length of these structures was measured by using 3 randomly selected microscopic images and analyzing them with the help of an "Angiogenesis Analyzer" plugin in ImageJ software (NIH, Bethesda, MD, USA) as described previously [Carpentier *et al.*, 2020; Onak Pulat *et al.*, 2021]. The obtained data of the experimental groups were normalized with the data of the control group and the change in the length of the tubular structures was represented as a percentage.

2.7 Cell Viability

At the end of the experimental procedures, the viability of HUVECs was analyzed by 3-(4,5-dimethythiazol-2-yl)-2,5-diphenyl tetrazolium bromide (MTT) on day 7. First, a 5 mg/ml stock solution was prepared. Then 10% of MTT solution and 90% of DMEM without serum were added to the cells. After 2 h of incubation, MTT solution was removed and 100 μL of Dimethyl Sulfoxide (DMSO) solution (Merck, Darmstadt, Germany) was added to the cells. After 30 minutes of incubation with DMSO, the absorbance values of the samples were measured at 570 nm with the microplate reader. Finally, the data obtained in this analysis were normalized with the data of the control group and the average percentages of the cell viabilities were calculated.

2.8 Intracellular ROS Generation

Light therapies such as PBM or PDT induce ROS production intracellularly and these molecules play a key role to provoke specific cellular functions inside the cells after these applications. For this, the amount of intracellular ROS production was analyzed by using a non-fluorescent probe of 2′,7′-dichlorofluorescein diacetate (DCFH-DA, Sigma-Aldrich, St. Louis, MO, USA) after light treatments. The available ROS molecules convert DCFH-DA into a fluorescent molecule of dichlorofluorescein (DCF). Before the light applications, the cells were incubated with 0.01 mM of DCFH-DA for 45 minutes. Afterward, the cells were washed twice with PBS and then the experimental procedures of PBM of low-PDT were applied. At the end of the applications, the fluorescence intensity of DCF was measured using the microplate reader directly with an excitation wavelength of 485/20 nm and an emission wavelength of 535/20 nm to determine the level of intracellular ROS production. The data obtained in each group were normalized with the data of the control group and the average percentages of the ROS levels were calculated.

2.9 NO Release

Light therapies, especially PBM, induce the release of NO molecules bound to mitochondria. For this, Griess reagent (Biotium, Fremont, CA, USA) was used to assess the amount of NO released. Griess reagent contains sulfanilic acid and N-(1-naphthyl)ethylenediamine and they react with nitrite, the breakdown product of NO. At the end of this reaction, a dye molecule is formed that can be measured spectrophotometrically. 24 hours after the light applications, an identical volume of Griess reagent and the supernatant solution from each sample were mixed and incubated for 30 minutes at room temperature. The absorbance values of each sample were measured using the microplate reader at a wavelength of 548 nm after each light application. The amount of nitrite in each sample was calculated using the standard curve formula as an indicator for the NO molecules released after the applications.

2.10 Mitochondrial Membrane Potential (MMP) Change

The changes in the MMP of the cells treated with light applications were determined by the JC-1-Mitochondrial Membrane Potential assay (Abcam, Cambridge, UK). The cells were rinsed with dilution buffer and then incubated with 0.01 mM of JC-1 solution for 10 minutes at 37°C before the light applications. Then the cells were washed twice with the dilution buffer and the appropriate application protocols were carried out in each PBM and PDT group. The fluorescent signals were read instantly at an excitation wavelength of 475 nm and the emission wavelengths of 595 nm and 535 nm with a microplate Reader (CLARIOstar Microplate Reader BMG LABTECH, Germany). Besides, the red signals of the live cells in each experimental group were captured with 20X magnification by using a fluorescent microscope (Olympus CKX41, Olympus Co. Ltd., Tokyo, Japan). CellSens Imaging Software was used to obtain these images where the red fluorescence represented the hyperpolarization of the live cells.

2.11 Immunofluorescence Staining

For the analysis of the angiogenesis induced by light therapies in HUVECs, immunofluorescence staining was performed for the angiogenesis-related proteins of vascular endothelial growth factor (VEGF), Platelet Endothelial Cell Adhesion Molecule-1 (PECAM-1), and von Willebrand factor (vWf). At the end of the 7-day follow-up, HUVECs were washed twice with PBS and then fixed with 4% paraformaldehyde (Sigma-Aldrich, St. Louis, MO, USA) at 4°C for 30 minutes. Afterward, samples were immersed with 0.1% Triton X-100 in PBS for 1 hour and blocked with 1.5% Bovine Serum Albumin (BSA) in PBS for 2 hours. The samples were then incubated with primary antibodies in PBS containing 1% BSA overnight at 4°C. Primary antibodies were VEGF (1:50, cat. no. sc-53462, Santa Cruz Biotechnology Inc., Santa Cruz, California, USA), PECAM-1 (1:50, cat. no. sc-376764, Santa Cruz Biotechnology Inc., Santa Cruz, California, USA) and vWf (1:50, cat. no. sc-365712, Santa Cruz Biotechnology Inc., Santa Cruz, California, USA). The fluorescent secondary antibody was m-IgGκ BP-PE (1:50, cat. no. sc-516141, Santa Cruz Biotechnology Inc., Santa Cruz, California, USA) and it was diluted with 1% BSA before use. Each sample was also stained with 4,6-diamidino- 2-phenylindole (DAPI) to image the cell nuclei. Using the inverted fluorescent microscope (Olympus CKX41, Tokyo, Japan), the immunofluorescent images of the expression patterns of VEGF, PECAM-1, and vWF proteins were captured with the same exposure time and light intensity.

2.12 Relative Expressions of vWf and PECAM-1 gene

On day 7 after all light irradiations were completed, the relative expressions of vWf and PECAM-1 gene were assessed with quantitative real-time PCR analysis. First, total RNA in the cells was isolated for each group using a total RNA purification kit (GeneAll Biotechnology, Co., Ltd., Seoul, Korea). Afterward, the conversion of the extracted/purified RNA to cDNA was performed using the HiScript III 1st Strand cDNA Synthesis Kit (Vazyme Biotech Co., Ltd, Nanjing, China). Finally, qRT-PCR analysis was performed with the obtained cDNAs by using the forward and reverse gene-specific primers. Glyceraldehyde 3-phosphate dehydrogenase (GAPDH) was used as a housekeeping gene. StepOne Plus Real-Time PCR System (Applied Biosystems, Foster City, USA) was used for the qRT-PCR process. The expression levels of each gene were analyzed according to the expression level of GAPDH with StepOne Software v2.3. The forward primer of GAPDH was GAAATCCCATCACCATCTTCC and the reverse primer of GAPDH was CCAGCATCGCCCCACTT, the forward primer of vWf was CCCATTTGCTGAGCCTTGT and the reverse primer of vWf was GGATGACCACCGCCTTTG, the forward primer of PECAM-1 was GCTGACCCTTCTGCTCTGTT and the reverse primer of PECAM-1 was TGAGAGGTGGTGCTGACATC (Oligomer, Ankara, Turkey).

2.13 Temperature Monitoring

During light therapies, the applied light energy may be converted into heat energy which may result in significant temperature increase and irreversible damage. Especially applications in the infrared regime and the presence of a photosensitizer are more prone to this outcome. For this, the temperature change was monitored with a thermal camera (Testo, Thermal imager). The measurements were performed during all light applications. The temperature was measured at the beginning and immediately at the endpoint of the light irradiation. The changes in temperatures were calculated.

2.14 Statistical Analysis

Each application was performed with at least three samples and repeated three times. The data obtained were first evaluated by one-way ANOVA. Then it was followed by Tukey's post hoc test using GraphPad Prism Version 9.0.1 software (GraphPad Software Inc., La Jolla, CA, USA). The p values less than 0.05 were considered statistically significant.

3. RESULTS

3.1 Cytotoxicity of ICG on HUVECs

Figure 1 shows the cell viability of HUVECs after 24 hours of incubation with different ICG concentrations. It was observed that ICG alone did not show any significant toxic effect. There was a slight decrease observed with the concentrations of 0.05, 0.1, 0.5, 1, and 2.5 μM. The concentrations of 0.25 and 5 μM ICG induced an increase in cell viability. However, there were no statistically significant differences between any experimental data and the control group (Figure 1). For low-dose PDT applications, 0.1 μM ICG was chosen because of being the possible lowest concentration which was capable to produce enough ROS for PBM, but not too much to kill the cells. The higher concentrations than 0.1 μM ICG may induce significant ROS production in the presence of light irradiation at 808-nm wavelength.

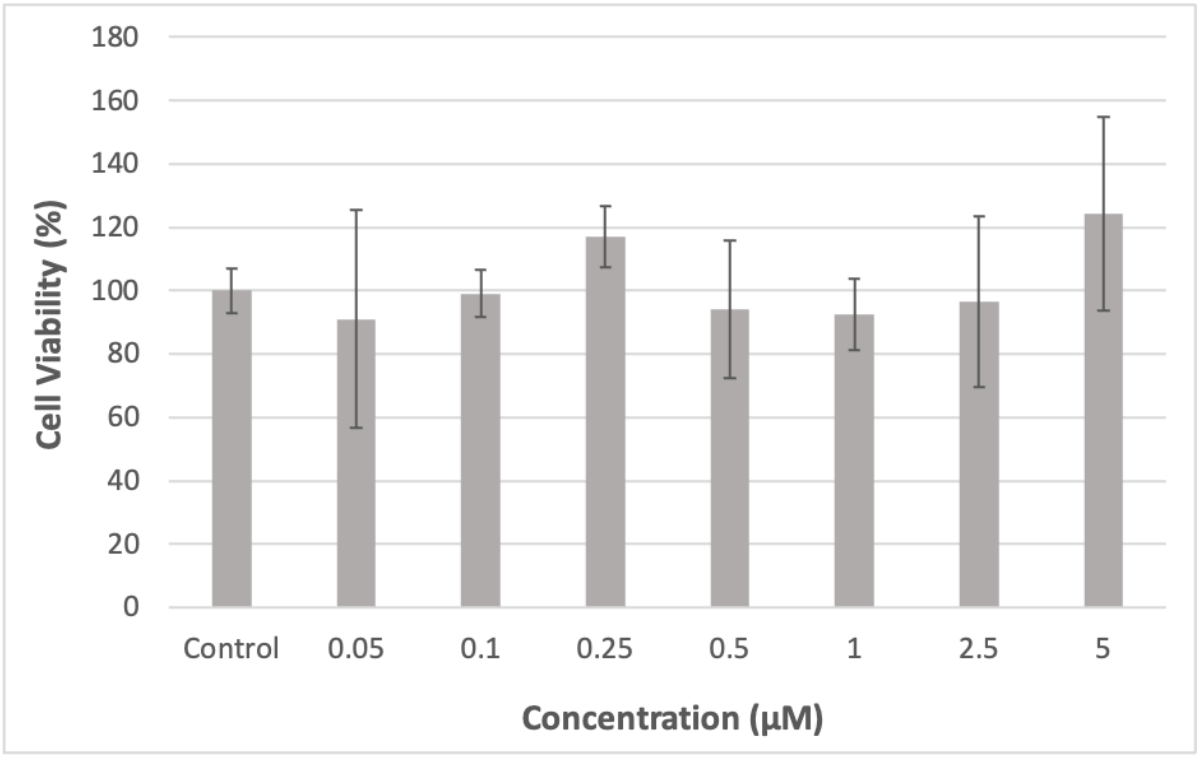

Figure 1. Cell Viability of HUVECs after the incubation with different ICG concentrations (0.05, 0.1, 0.25, 0.5, 1, 2.5, and 5 μM). Each column represents the average of the normalized data ± standard deviation ($n > 8$).

3.2 Cell Viability after PBM and Low-Dose PDT applications

The cell viability analysis of HUVECs was carried out at the end of the 7-day follow-up period according to the metabolic activity of the live cells determined by the MTT assay. As shown in Figure 2.a., there is an increase of approximately 3% after a single light treatment of PBM. The value increased to 7% after triple treatment of PBM. Figure 2.b. shows that the increase in cell viability was 5% after a single treatment of PDT and this value increased to 20% after triple treatment of PDT. Low-dose PDT resulted in clearly higher cell viability than PBM did for both treatment modalities. The outcomes of all triple treatments were statistically significant compared to the control group. Besides, the single treatment of PDT application was also significantly different from the control group. Single and triple ICG applications did not change the cell viability significantly. Only a slight decrease was observed in these groups after these applications (Figure 2).

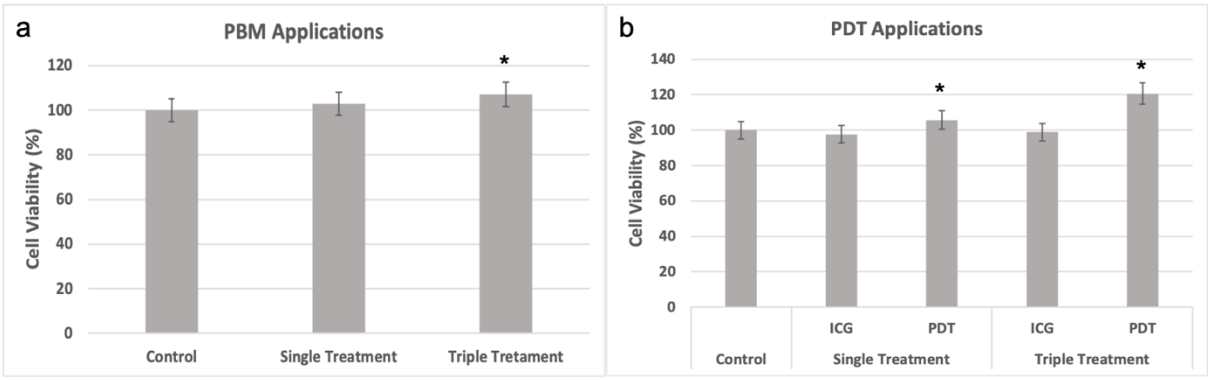

Figure 2. Cell viability analysis of HUVECs a) after PBM applications (single and triple treatment) and b) after only ICG and PDT applications (single and triple treatment) on the 7th day. Energy density was 1 J/cm^2, and ICG concentration was 0.1 μM. Each column represents the average of the normalized data ± standard deviation (n > 8). * symbolizes significant differences compared to the control group, p<0.05.

3.3 Morphological Analysis of HUVECs after Light Treatments

Figures 3, 4, and 5 show microscopic images of the cells after single and triple treatments of PBM, low-dose PDT, and ICG, respectively. It was observed that HUVECs successfully proliferated and elongated in PBM and low-dose PDT groups with respect to the control group. Especially the density of the cells irradiated with light three times was higher than the cells treated once or in the control group (Figures 3 and 4). As it was shown in Figure 5, single and triple ICG applications did not induce any change on HUVECs in terms of proliferation and elongation. There were no clearly observable connections and elongations between the cells treated with ICG. It can also be clearly observed that the cell density was higher and the conditions of the cells were better in the control group compared to the cells in ICG groups. (Figure 5).

These images were analyzed by the Angiogenesis Analyzer plugin of ImageJ software to measure the lengths of tube-like structures. As it is shown in Figure 6.a., the average length of endothelial cell tubular structure was increased to 111± 2% in PBM, whereas there was an 8% decrease in the average length of tube-like structures of PDT groups after a single treatment. The average length of tubular structures was measured as 100±4% after a single ICG application. After triple treatments, the lengths of endothelial cell tubular structures were measured as 110 ± 2% in the PBM group, 118 ± 3% in the PDT group, and 98±2% in the ICG group (Figure 6.b.). All the changes in the lengths of tube-like structures obtained with PBM or PDT applications were statistically significant compared to the control group. However, the outcomes of the ICG groups were not statistically significant compared to the control group (Figure 6).

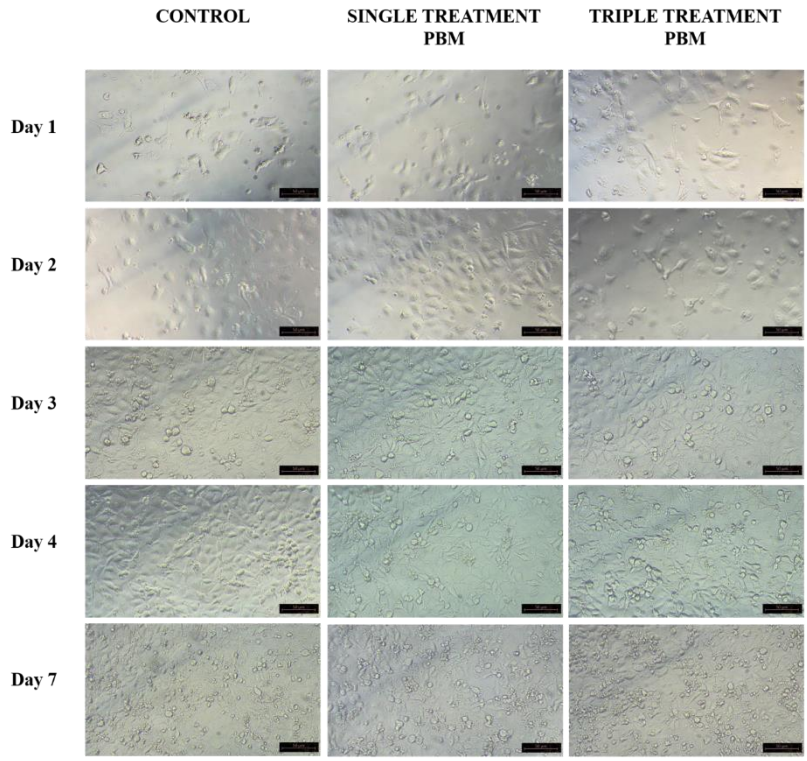

Figure 3. Microscopic images of HUVECs were obtained after single and triple PBM treatments on days 1, 2, 3, 4, and 7. Scale bar: 50 μm.

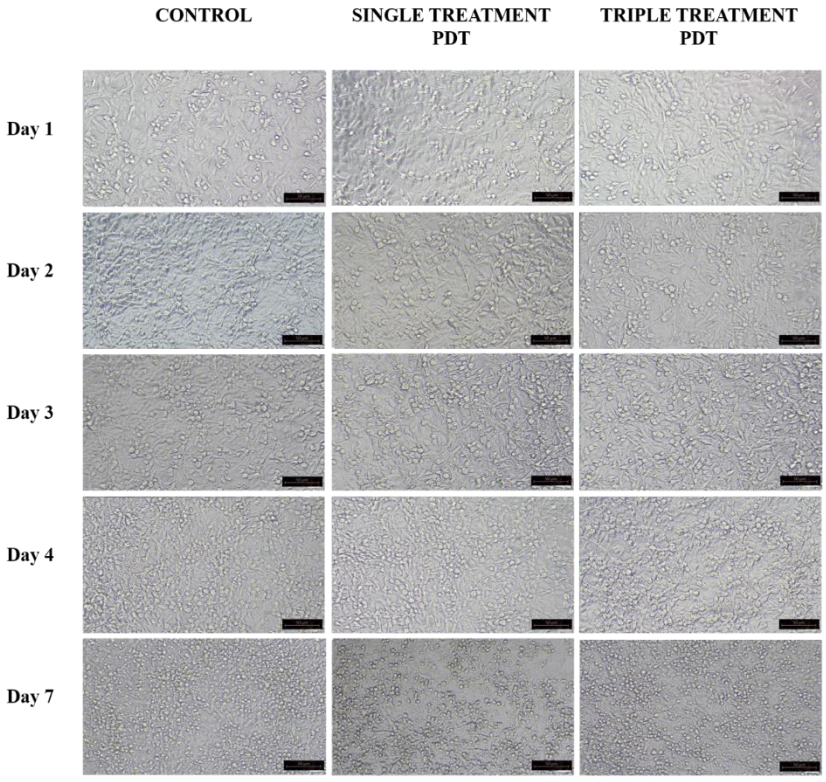

Figure 4. Microscopic images of HUVECs were obtained after single and triple low-dose PDT treatments on days 1, 2, 3, 4, and 7. Scale bar: 50 μm.

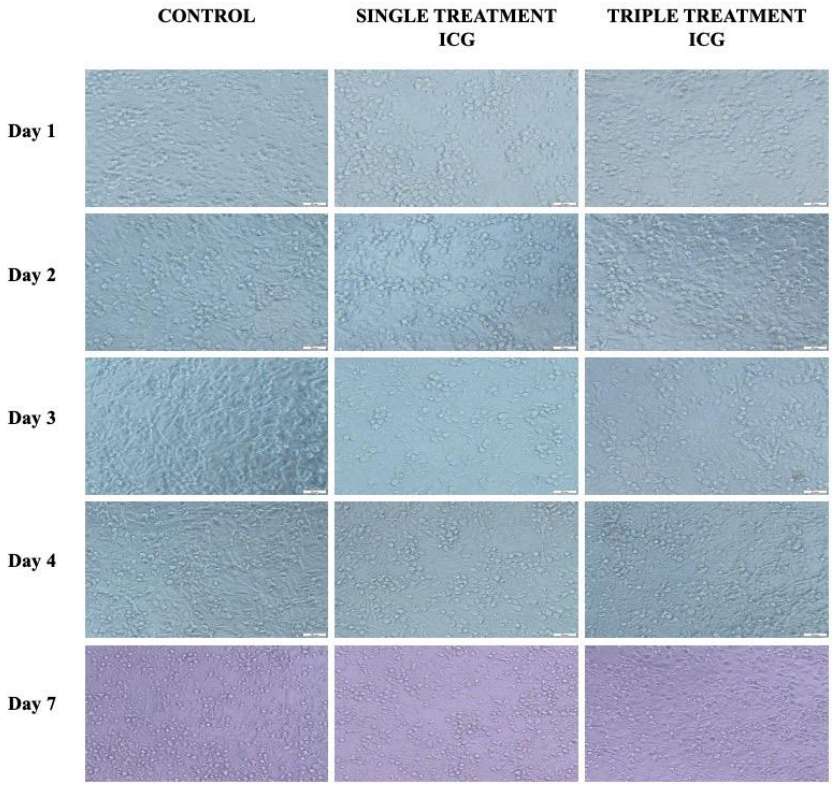

Figure 5. Microscopic images of HUVECs were obtained after single and triple ICG applications on days 1, 2, 3, 4, and 7. Scale bar: 50 μm.

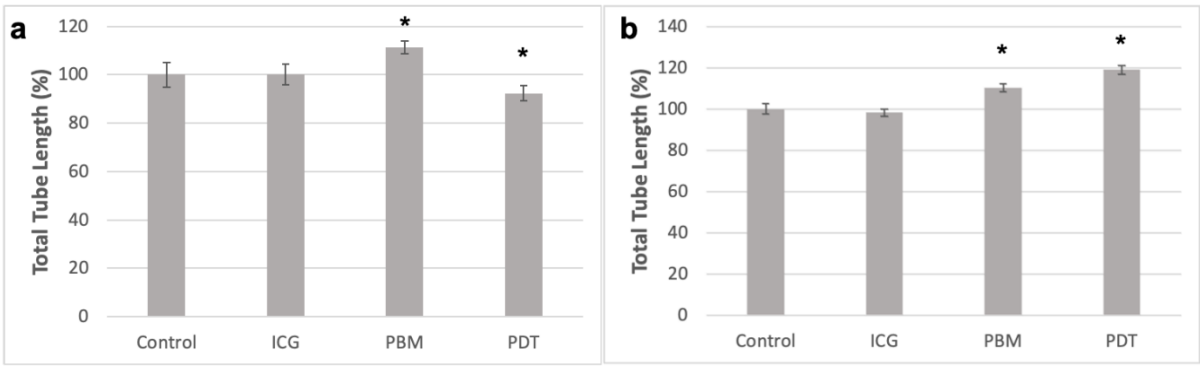

Figure 6. The total length of the tubular structures after a) single treatment of ICG, PBM, and low-dose PDT, b) triple treatment of ICG, PBM, and low-dose PDT on day 7. Each column represents the average of the normalized data ± standard deviation (n > 8). * symbolizes significant differences compared to the control group, $p<0.05$.

3.4 Intracellular ROS Generation

The intracellular ROS analysis shows that, surprisingly, low-dose PDT application caused a clear drop after the first treatment, while a single treatment of PBM did not cause a significant change in ROS level compared to the control group. After the second light treatment, both PBM and PDT application did not change the ROS level. The measured amounts were quite similar to the amounts in the control group. After the third light treatment, a slight increase was observed in both applications. This increase was higher in PDT which was approximately 10%, but it was less than 10% in PBM (Figure 7).

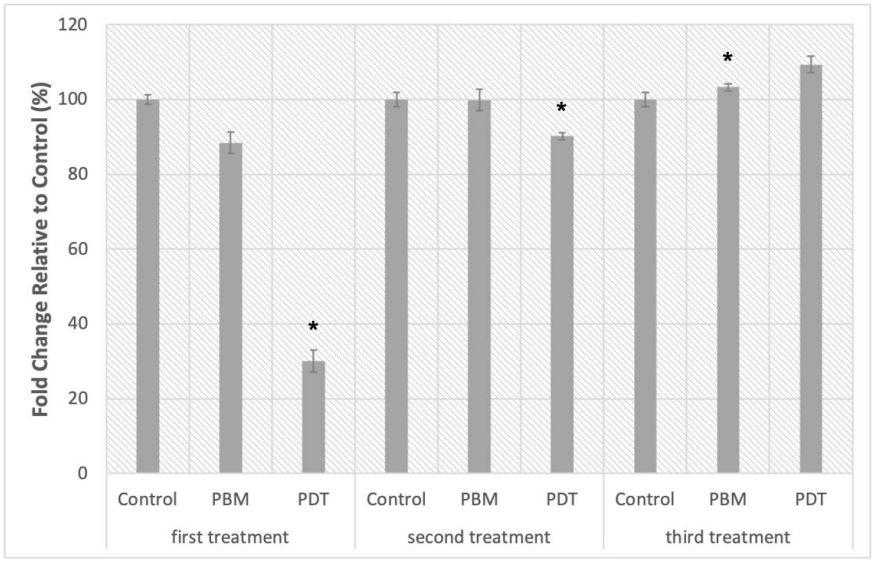

Figure 7. Intracellular ROS analysis in PBM and PDT groups after each light treatment. Each column represents the average of the normalized data ± standard deviation (n > 8). * symbolizes significant differences compared to the control group, $p<0.05$.

3.5 NO Release

The levels of NO released after the light applications were quite remarkable as shown in Figure 8. The level of NO released in PBM was nearly 4 times higher than that of the control and PDT groups after the first light application. The first application of PDT did not cause a significant NO release. After the second light application, surprisingly, the level of released NO in PBM decreased drastically back down to half of the value of the control group, whereby the level of released NO in PDT was nearly 4.5 times higher than that of the control group. After the last light application, the level of released NO in PBM was quite similar to the control group, whereby the level of released NO in the PDT group was still nearly 4.5 times higher than that of the control group and almost the same as the amount released after the second light application (Figure 8).

3.6 Mitochondrial Membrane Potential change

Figure 9 shows the fluorescent images of hyperpolarization in the mitochondria of HUVECs after light treatments. The intensity of red fluorescence in PBM and PDT was quite higher than in the control group and it became more intense day by day after other light applications (Figure 9).

Figure 10 shows the fluorescence intensity ratio calculated from the fluorescent intensities measured at 535 nm (for depolarization) and 595 nm (for hyperpolarization). On the first day, immediately after the light application, the mitochondrial membrane potential change was almost the same in PBM and PDT groups. It was an approximately 15% increase compared to the control group and an indication of hyperpolarization. After the second light treatment, the change in MMP for PDT was slightly higher than the value of PBM and it was still an increase up to 10% which was an indication of hyperpolarization. After the third light application, the increases in MMP change for both modalities were nearly 20% which still showed the hyperpolarization of HUVECs and with this application, the highest values in MMP change were reached (Figure 10).

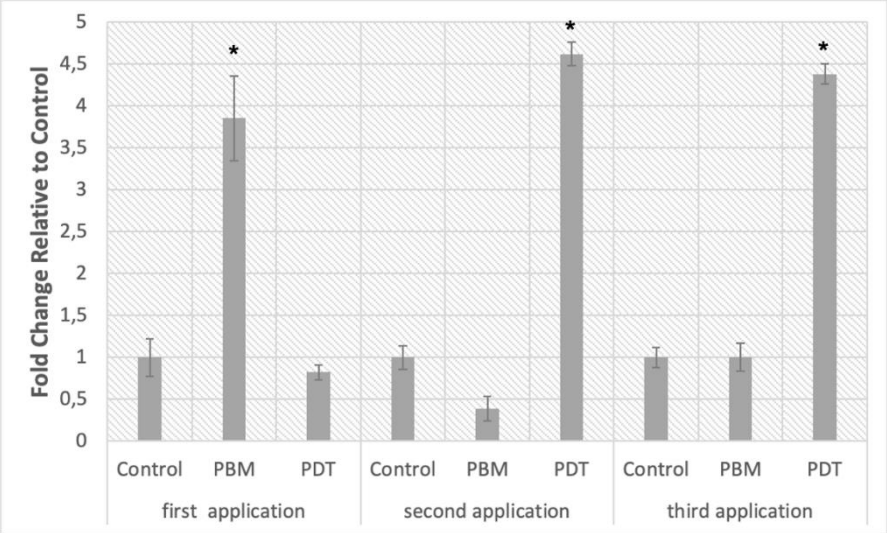

Figure 8. NO release in PBM and PDT groups after each light application. Each column represents the average of the normalized data ± standard deviation (n > 8). * symbolizes significant differences compared to the control group, $p<0.05$.

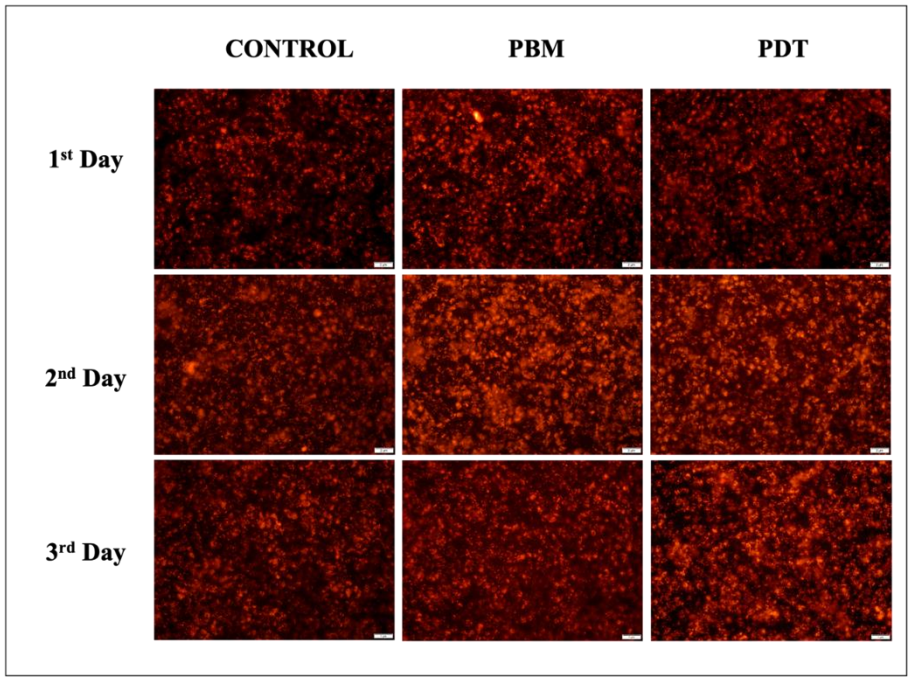

Figure 9. Hyperpolarization images of HUVECs depending on the mitochondrial membrane potential change after PBM and low-dose PDT applications on days 1, 2, and 3. The scale bar is 50 μm.

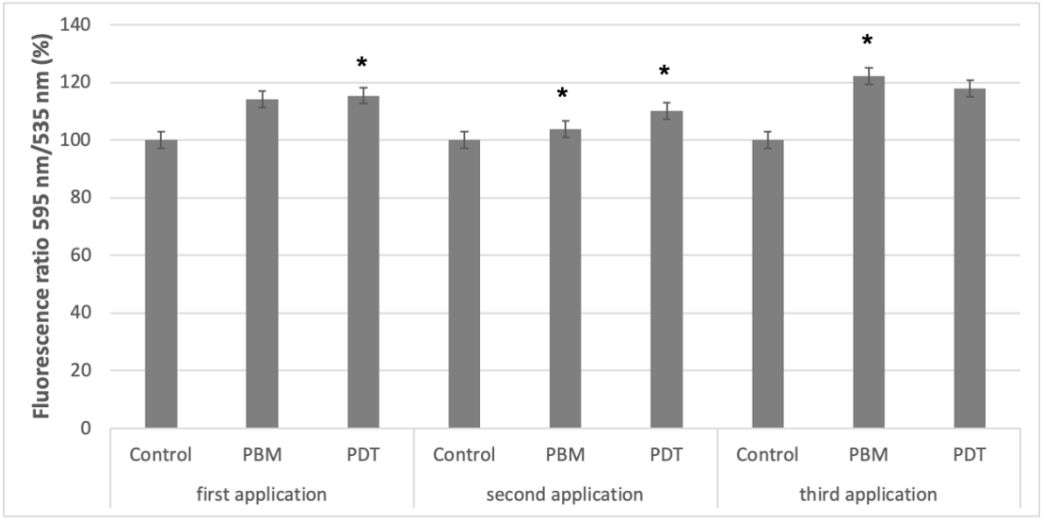

Figure 10. Mitochondrial Membrane Potential Change after each light application in PBM and PDT groups. Each column represents the average of the normalized data ± standard deviation (n > 8). * symbolizes significant differences compared to the control group, $p<0.05$.

3.7 Immunofluorescent Staining

Immunofluorescence staining of HUVECs was done on day 7 after single and triple treatments were performed on both groups, PBM and PDT. The images of the VEGF, PECAM-1, and vWf proteins had red color and the nuclei of the cells had blue-colored DAPI staining. The red color for each protein can be seen in each group, with different intensities as shown in Figure 11. It can be observed that vWf in the single-treated groups was weaker in staining compared to the triple-treated groups. The intensity of the red color for vWf protein in triple-treated low-dose PDT was significantly stronger than PBM. Similar outcomes were obtained for PECAM-1 and VEGF proteins. The expressions of PECAM-1 and VEGF were higher in triple-treated light applications. Low-dose PDT applications induced higher expressions of these proteins compared to PBM applications. The expressions of all these proteins were higher in the experimental groups compared to the control (Figure 11).

3.8 Relative Expressions of vWf and PECAM-1 gene

qRT-PCR analysis was performed for the vWf and PECAM-1 gene at the end of the 7-day follow-up for each group. As shown in Figure 12, all light applications whether they were single or triple, PBM or PDT, resulted in higher expressions of vWf and PECAM-1 gene compared to the control group. These genes were more highly expressed in triple-treated groups than in the single-treated groups. Besides, low-dose PDT applications were more successful to induce the higher expressions of these genes than PBM applications were. Furthermore, none of these applications were statistically significant compared to the control group.

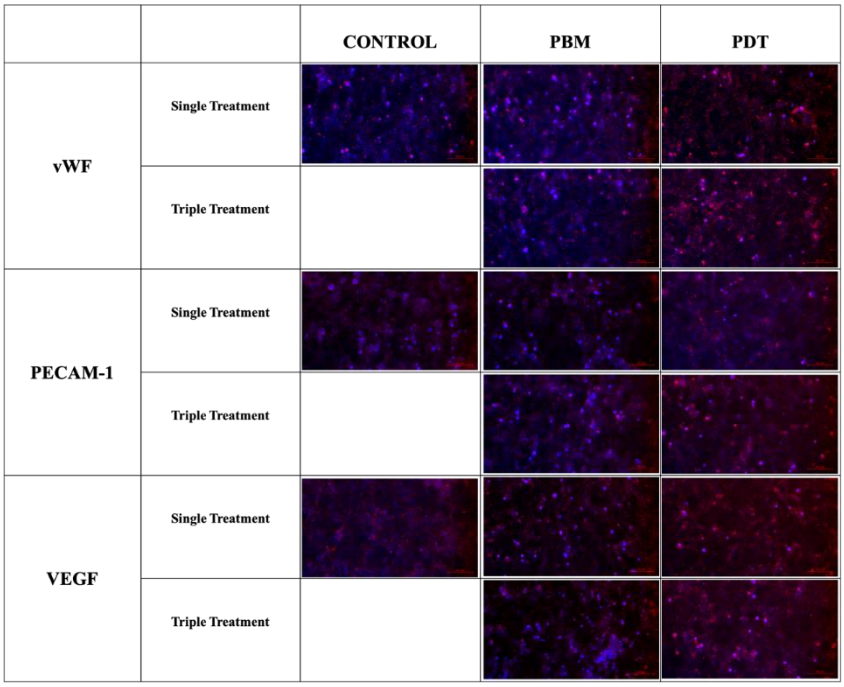

Figure 11. The microscopic images of the immunofluorescence staining of HUVECs in control, PBM, and low-dose PDT groups for vWf, PECAM-1, and VEGF proteins on day 7.

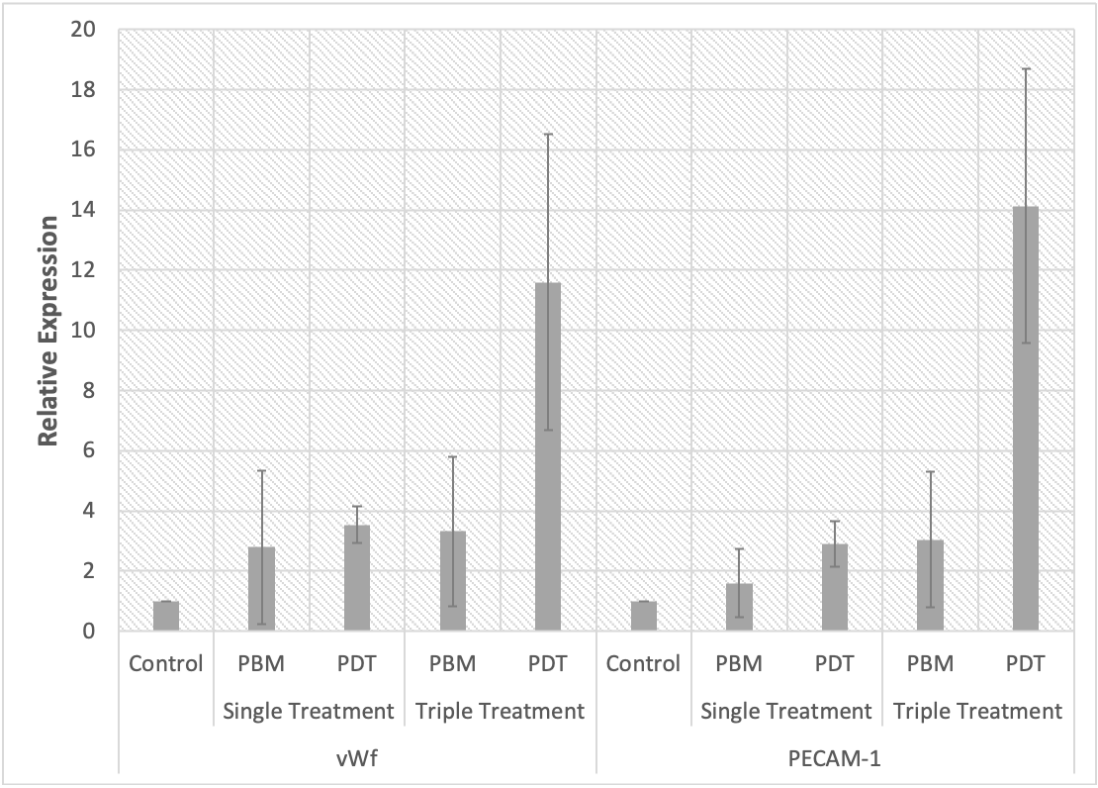

Figure 12. qRT-PCR analysis of PECAM-1 and vWF gene in the control, PBM, and low-dose PDT groups on day 7. Each column represents the average of the normalized data ± standard deviation ($n > 8$).

3.9 Temperature Monitoring

In each light application, the temperature changes were monitored and only a little increase of approximately 0.2°C was observed as shown in Table 1. The combination of ICG and near-infrared light did not cause a significant temperature increase.

Table 1. Temperature measurements during light applications.

	1st Light Application		2nd Light Application		3rd Light Application	
	PBM	**PDT**	**PBM**	**PDT**	**PBM**	**PDT**
Start (ºC)	29.6	30	30.2	31	31.2	31
End (ºC)	29.8	30.1	30.4	31.2	31.4	31.2
Δt (ºC)	0.2	0.1	0.2	0.2	0.2	0.2

4. DISCUSSION

This study comparatively analyzed the effectiveness of PBM and low-dose PDT on HUVECs towards vascularization and tried to reveal what happens if the light treatment was performed more than once. First, the appropriate ICG concentration was determined for low-dose PDT application to prevent any possible cytotoxic effect of ICG. It was seen that ICG was quite a safe photosensitizer and it can be used for this purpose. Among the ICG concentrations investigated in the cytotoxicity analysis, the possible lowest concentration, which was capable to produce enough ROS for PBM, but not too much to kill the cells, was chosen. With the concentration of 0.05 μM, there was a possibility to be very low and even not induce any significant cellular mechanism. Higher concentrations analyzed in this study may have the risk of causing cell death. Thus, 0.1 μM ICG was chosen for low-dose PDT applications. Even though it exhibited a decrease in cell viability, it cannot be regarded as a cytotoxic concentration. To achieve a certain amount of ROS production enough for biostimulation after light applications, but not to cause any detrimental effect which is related to a higher amount of ROS, 0.1 μM ICG seemed quite safe to use in PDT for biostimulative purposes. Another important parameter in low-dose PDT application was the energy density which should be properly optimized and not cause any significant thermal damage depending on the absorption of NIR light by cells/tissue [Ateş *et al*., 2018; Khorsandi *et al*., 2021]. According to the information in the literature, 1 J/cm^2 energy density was determined and used in PBM and low-dose PDT applications [Topaloglu and Bakay, 2022; Bölükbaşı Ateş *et al*., 2020; Ateş *et al*., 2017]. During all light treatments, the temperature change was monitored with a thermal camera and it was observed that only 0.2°C change was obtained at most, even in the presence of ICG which is a strong absorber of NIR light [Topaloglu *et al*., 2015]. This result proved that the mechanisms of PBM or low-dose PDT applications with these parameters did not depend on the photothermal interaction mechanism and there was no risk for a thermal side-effect. Then the effects of ICG, PBM, and low-dose PDT applications were analyzed on cell proliferation. The increase in the metabolic activity of HUVECs was not high after any light application, even after the triple light treatment. The maximum increase was 20% which was obtained after the triple light treatment of low-dose PDT. Nevertheless, it was still significantly different from the control group. Only ICG applications, whether it was applied once or thrice, did not cause any significant change in the cell viability at the end of 7 days. It was clearly observed that ICG alone did not have the possibility to stimulate cell proliferation without light irradiation.

The morphological analysis of HUVECs which was performed on days 1, 2, 3, 4, and 7 also confirmed the increase in cell viability day by day for all light-treated groups. When the images obtained from single or triple light-treated groups were compared, the triple light treatment provided more positive effects on the cell viability. Besides, tube-like structure formation can also be visualized in microscopic images. After single light treatment, PBM promoted a better tubular structure formation compared to low-dose PDT application. After triple light treatments, low-dose PDT promoted a better tubular structure formation compared to PBM application. Nevertheless, PBM or low-dose PDT applications, whether they were applied once or thrice, provided more and longer tubular structures than the control group. Thus, it can

be said that both of these applications were successful at the differentiation of HUVECs. After only ICG applications, similar outcomes were obtained with the analysis of tubular structures as cell viability analysis. Whether ICG was applied once or thrice, it did not cause any significant change in the length of the tubular structures at the end of 7 days. The lengths of these structures in this group were similar to the lengths that were obtained in the control group. It was understood that ICG alone did not stimulate tubular structure formation without light irradiation.

To understand the action mechanism of these applications on cell differentiation, some mechanistic analyses were performed. One of the important molecules in these mechanisms is ROS which has a key role in many biological processes [Schieber and Chandel, 2014]. Thus, it was assumed that the production of intracellular ROS might have become predominant after these applications. Surprisingly, the detected intracellular ROS production was very low in low-dose PDT application after single light treatment. Besides, the amount of intracellular ROS in both PBM and low-dose PDT groups was lower than the amount measured in the control group. After the second light treatment, the amount of ROS increased to a certain extent but was still lower than the amount in the control group. After the third light treatment, its amount became higher than the control group for both applications. This outcome showed the importance of the light treatments applied more than once and it also correlated with the findings of the increases in cell viability and tube-like structure formation obtained after triple light treatment in PBM and low-dose PDT applications. When PDT was used to destroy pathogenic or cancer cells, a higher amount of intracellular ROS was produced with higher photosensitizer concentrations and light doses. The amount of ROS may become 5 times higher than that of the control group [Topaloglu *et al*., 2021b]. When PDT was used at low-level for biostimulative purposes, Topaloglu *et al*. found that the increase in the amount of intracellular ROS produced after repeated low-dose PDT applications was around 10-20% [Topaloglu and Bakay, 2022] which was similar to the outcome obtained in this study. Thus, it can be said that lower photosensitizer concentration and light doses used in this study induced a similar amount of ROS production to the amount obtained in previous low-dose PDT studies.

NO release is an indication of PBM and as a signaling molecule, it has a key role to regulate some reactions ending up with some major outcomes of stimulative actions of light [Topaloglu and Bakay, 2022]. Thus, NO release was immediate with the first light application of PBM and the detected amount was more than 4-fold that of the amount in the control group. Similarly, the increase in cell viability and tubular structures obtained in PBM application was higher after the first light treatment, which proved the role of NO release in this mechanism. Later on, the amount of NO release was decreased until the value in the control group after the second and third light applications of PBM. We understood that the action mechanism of PBM was faster at first and it became slower in the upcoming treatments. On the other hand, the amount of NO release was nearly the same as the amount of NO in the control group after the first light application. After the second and third light applications of low-dose PDT, the amount of NO release was 4.5 times higher than that of the control group. The remarkable changes in this analysis were obtained after repeated light application for low-dose PDT. It also confirmed the results obtained after PDT applications in the previous analysis. It was understood that the action mechanism of PDT occurs slowly, but became more impactful on the differentiation of HUVECs. In previous PDT applications that aimed to destroy cancer cells, no significant change in NO release was observed when the photosensitizer concentration and light dose were used at a high level. The mechanism of the traditional PDT applications depends on the production of intracellular ROS which is toxic to the cells [Topaloglu *et al*., 2021b]. In previous low-dose PDT studies, the amount of NO release obtained was similar to the outcomes obtained in this study. Topaloglu *et al*. obtained a nearly 50% increase in NO release when PDT application was used at a low level to induce neural cell differentiation [Topaloglu and Bakay, 2022]. However, the increase in NO release was more remarkable in this study, which was more than 4-fold that of the control group.

In the mechanism of PBM, light is absorbed directly by the mitochondria. This situation causes a proton gradient across the mitochondrial membrane. Related to this phenomenon, the biostimulation reactions end up with the hyperpolarization of the mitochondria which is related to the increase in cell viability. When cell death occurs, depolarization is observed [Topaloglu and Bakay, 2022]. To understand

the mechanism of PBM and low-dose PDT in this study, the MMP changes in HUVECs were visualized by a JC-1 probe for hyperpolarization/depolarization. As it was shown in Figure 9, hyperpolarization was more apparent in the experimental groups compared to the control group. As expected, a higher increase in MMP was observed after the single treatment of PBM application. The reason for this outcome should be the absorption of light directly by the COX of mitochondria in PBM applications [Topaloglu *et al*., 2021a]. The changes in MMP continued with the consecutive light applications and low-dose PDT provided the same results as PBM did. It showed the importance of the triple light treatment to stimulate the cells continuously and to get more successful results in terms of cell differentiation. Besides, there was no indication of depolarization in the mitochondrial membrane which is related to cell death. This was the proof for PDT applications that did not induce any cell death mechanism, such as apoptosis.

HUVECs can form tube-like structures by expressing angiogenesis-related proteins such as VEGF, PECAM-1, and vWf [Müller *et al*., 2002; Yaralı *et al*., 2020]. Previous studies that examined the effect of red and near-infrared light on the expressions of the angiogenic markers showed that these wavelengths induced the expression of VEGF [Cury *et al*., 2013; Basso *et al*., 2013]. Similar results were obtained in this study, too. Immunofluorescence staining provided the findings of the increase in the expressions of vWf, PECAM-1, and VEGF. The expressions of these proteins in PBM and low-dose PDT applications were greater than in the control group. qRT-PCR analysis of the genes that express vWf, PECAM-1, and VEGF proteins confirmed the results of immunofluorescence staining. In qRT-PCR analysis, the expressions of the vWf and PECAM-1genes were evaluated and in general overexpression of these genes was observed compared to the control group. Especially, the highest increases for both genes were obtained after the triple light treatment of PDT applications. This finding was in parallel with the findings of other analyses. In terms of cell viability, tube-like structure formation, intracellular ROS production, and NO release, the highest changes were always obtained after the triple light applications of low-dose PDT.

5. CONCLUSIONS

Light therapies have numerous beneficial effects. Biphasic dose-response of the cells towards therapeutic light applications broadens the fields and the purposes of the use of light in medicine [Topaloglu and Bakay 2022]. With the outcomes of this study, it can be concluded that PBM and low-dose PDT applications promote the vascularization of HUVECs. Thus, they can be a valuable tool in tissue engineering to accelerate the wound healing process. Besides, it was seen that PDT, which is commonly used to treat cancer and infection [Topaloglu *et al*., 2021b], may also fasten cell proliferation/differentiation, wound healing, pain relief, etc. via some biochemical reactions inside the cells by keeping the parameters at low level [Topaloglu and Bakay 2022]. In this study, the therapeutic outcomes of PBM and low-dose PDT applications on HUVECs were quite similar to each other. Both of them were successful to induce tube-like structure formation. Nevertheless, low-dose PDT exhibited a little bit more effective result. Inducing the cellular mechanisms responsible for vascularization and the behavior of signaling molecules such as ROS or NO with the use of a photosensitizer and its excitation by an appropriate wavelength seems to be more effective in biostimulation, instead of provoking mitochondria in PBM. Besides, these light therapies were applied in two different modalities which were single and triple treatments in this study. Triple light treatments for both PBM and low-dose PDT showed better results, meaning that consecutive light treatments cause further impulses resulting in ongoing changes in cellular metabolism. We can also add that 808-nm of wavelength was also beneficial in inducing vascularization and did not cause any thermal side-effect which is very likely to occur in the infrared (IR) region, even in the presence of ICG. ICG, as a photosensitizer, did not induce a significant cytotoxic effect on HUVECs. Thus, they can be safely used without causing any harmful effects on the cells. Since vascularization is a big challenge in tissue engineering, these therapeutic light applications offer a safe way to improve and accelerate the wound healing process and the vascularization of the implanted tissue.

6. ACKNOWLEDGEMENT

This study was supported by İzmir Katip Çelebi University Scientific Research Project (2021-TYL-FEBE-0001). The authors are grateful to Emel Bakay, Assoc. Prof. Utku Kürşat Ercan, Assist. Prof. Didem Şen Karaman, and Assoc. Prof. Ozan Karaman for their valuable contributions.

REFERENCES

Amaroli, A. et al., 2019, "Photobiomodulation with 808-nm diode laser light promotes wound healing of human endothelial cells through increased reactive oxygen species production stimulating mitochondrial oxidative phosphorylation", Lasers in Medical Science, Vol. 34, Nr. 3, pp. 495.

Ateş, G. B. et al., 2018, "Indocyanine green-mediated photobiomodulation on human osteoblast cells", Lasers in Medical Science, Vol. 33, Nr. 7, pp. 1591–1599.

Ateş, G. B. et al., 2017, "Methylene blue-mediated photobiomodulation on human osteoblast cells", Lasers in Medical Science, Vol. 32, pp. 1847-1855.

Basso, F. G. et al., 2013, "Biostimulatory effect of low-level laser therapy on keratinocytes in vitro", Lasers in Medical Science, Vol. 28, Nr. 2, pp. 367–374.

Beltrán, B. et al., 2000, "The effect of nitric oxide on cell respiration: A key to understanding its role in cell survival or death", Proceedings of the National Academy of Sciences, Vol. 97, Nr. 26, pp. 14602–14607.

Borutaite, V. et al., 2000, "Reversal of nitric oxide-, peroxynitrite- and S-nitrosothiol-induced inhibition of mitochondrial respiration or complex I activity by light and thiols", Biochimica et Biophysica Acta. Bioenergetics, Vol. 1459, Nr. 2–3, pp. 405–412.

Bölükbaşı Ateş, G. et al., 2020, "Photobiomodulation effects on osteogenic differentiation of adipose-derived stem cells", Cytotechnology Vol. 72, pp. 247-258.

Carpentier, G. et al., 2020, "Angiogenesis Analyzer for ImageJ — A comparative morphometric analysis of "Endothelial Tube Formation Assay" and "Fibrin Bead Assay"", Scientific Reports, Vol. 10, Nr. 11568.

Castano, A. P. et al., 2004, "Mechanisms in photodynamic therapy: part one-photosensitizers, photochemistry and cellular localization", Photodiagnosis and Photodynamic Therapy, Vol. 1, Nr. 4, pp. 279–293.

Cury, V. et al., 2013, "Low level laser therapy increases angiogenesis in a model of ischemic skin flap in rats mediated by VEGF, HIF-1α and MMP-2", Journal of Photochemistry and Photobiology B: Biology, Vol. 125, pp. 164–170.

de Freitas, L. F., Hamblin, M. R., 2016, "Proposed mechanisms of photobiomodulation or low-level light therapy", IEEE Journal of Selected Topics in Quantum Electronics, Vol. 22, Nr. 3, pp. 348-364.

Hamblin, M. R., 2018, "Mechanisms and mitochondrial redox signaling in photobiomodulation", Photochemistry and Photobiology, Vol. 94, Nr. 2, pp. 199–212.

Hawkins, D. et al., 2005, "Low level laser therapy (LLLT) as an effective therapeutic modality for delayed wound healing", Annals of the New York Academy of Sciences, Vol. 1056, Nr. 1, pp. 486–493.

Hough, M. A. et al., 2014, "NO binding to the proapoptotic cytochrome c-cardiolipin complex", Vitamins and Hormones, Vol. 96, pp. 193–209.

Huang, Y. Y., (2009), "Biphasic dose response in low level light therapy", Dose Response, Vol. 7, Nr. 4, pp. 358-83.

Karu, T. I. et al., 2005, "Cellular effects of low power laser therapy can be mediated by nitric oxide", Lasers in Surgery and Medicine, Vol. 36, Nr. 4, pp. 307–314.

Khorsandi, K. et al., 2021, "Low-dose photodynamic therapy effect on closure of scratch wounds of normal and diabetic fibroblast cells: An in vitro study", Journal of Biophotonics, Vol. 14, Nr. 7, e202100005.

Mittal, M. et al., 2014, "Reactive oxygen species in inflammation and tissue injury", Antioxidants & Redox Signaling, Vol. 20, Nr. 7, pp. 1126–1167.

Müller, A. M. et al., 2002, "Expression of the endothelial markers PECAM-1, vWf, and CD34 in vivo and in vitro", Experimental and Molecular Pathology, Vol. 72, Nr. 3, pp. 221–229.

Onak Pulat, G. et al., 2021, "Role of functionalized self-assembled peptide hydrogels in in vitro vasculogenesis", Soft Matter, Vol. 17, pp. 6616–6626.

Schieber, M., Chandel, N. S., 2014, "ROS function in redox signaling and oxidative stress", Current biology: CB, Vol. 24, Nr. 10, pp. R453–R462.

Sibata, C. H. et al., 2000, "Photodynamic therapy: a new concept in medical treatment", Brazilian Journal of Medical and Biological Research, Vol. 33, Nr. 8, pp. 869–880.

Terena, S. M. L. et al., 2021, "Photobiomodulation alters the viability of HUVECs cells", Lasers in Medical Science Vol. 36, pp. 83-90.

Topaloglu, N. et al., 2015, "Antibacterial photodynamic therapy with 808-nm laser and indocyanine green on abrasion wound models", Journal of Biomedical Optics, Vol. 20, Nr. 2, 028003.

Topaloglu, N. et al., 2016, "The role of reactive oxygen species in the antibacterial photodynamic treatment: photoinactivation vs proliferation", Letters in Applied Microbiology, Vol. 62, Nr. 3, pp. 230-236.

Topaloglu, N. et al., 2021a, "Comparative analysis of the light parameters of red and near-infrared diode lasers to induce photobiomodulation on fibroblasts and keratinocytes: An in vitro study", Photodermatology, Photoimmunology & Photomedicine, Vol. 37, pp. 253-262.

Topaloglu, N. et al., 2021b, "Induced photo-cytotoxicity on prostate cancer cells with the photodynamic action of toluidine Blue ortho", Photodiagnosis and Photodynamic Therapy, Vol. 34, Nr. 102306.

Topaloglu, N., Bakay, E., 2022, "Mechanistic approaches to the light-induced neural cell differentiation: Photobiomodulation vs Low-Dose Photodynamic Therapy", Photodiagnosis and Photodynamic Therapy, Vol. 37, Nr. 102702.

Yaralı, Z. B. et al., 2020, "Effect of integrin binding peptide on vascularization of scaffold-free microtissue spheroids", Tissue Engineering and Regenerative Medicine, Vol. 17, Nr. 5, pp. 595–605.

Zhang, J. et al., 2016, "ROS and ROS-mediated cellular signaling", Oxidative Medicine and Cellular Longevity, Vol. 4350965.

Zhang, X. et al., 2005, "Low-dose photodynamic therapy increases endothelial cell proliferation and VEGF expression in nude mice brain", Lasers in Medical Science, Vol. 20, Nr. 2, pp. 74–79.

Zorov, D. B. et al., 2014, "Mitochondrial reactive oxygen species (ROS) and ROS-induced ROS release", Physiological Reviews, Vol. 94, Nr. 3, pp. 909–950.